

# Electrochemical and electrochromic properties of nanoworm-shaped Ta<sub>2</sub>O<sub>5</sub>–Pt thin-films

Kyung-Won Park<sup>a,\*</sup>, Michael F. Toney<sup>b,\*</sup>

<sup>a</sup> Department of Chemistry, The Pennsylvania State University, 104 Chemistry Building, University Park, PA 16802, USA

<sup>b</sup> Stanford Synchrotron Radiation Laboratory, Stanford Linear Accelerator Center, Menlo Park, CA 94025, USA

Received 9 November 2004; received in revised form 1 December 2004; accepted 6 December 2004  
Available online 24 December 2004

## Abstract

A Ta<sub>2</sub>O<sub>5</sub>–Pt nanostructure electrode was fabricated by means of cosputtering deposition method. Worm-like Pt nanoparticles were produced in Ta<sub>2</sub>O<sub>5</sub> matrix as observed by transmission electron microscopy (TEM) and small angle X-ray scattering (SAXS). The electrochemical and electrochromic properties of nanoworm-shaped Ta<sub>2</sub>O<sub>5</sub>–Pt electrode are compared with those of Ta<sub>2</sub>O<sub>5</sub> thin-film electrode without Pt nanoparticles.

© 2004 Elsevier B.V. All rights reserved.

**Keywords:** Proton transfer; Electrochromism; Ta<sub>2</sub>O<sub>5</sub>; Pt nanophases; Nanocomposite

## 1. Introduction

Nanostructured materials are attractive due to the particular fundamental properties that are present in such low-dimensional systems, which have unique properties different from those found in bulk scale. Research on nanostructures provides the potential for a variety of chemical, electronic, catalytic, electrochemical, and photonic applications [1–4]. The electrical, optical and magnetic properties of nanostructures vary with factors such as size, shape and crystallinity. In particular, nanophase composite structures, which consist of nanoparticles in a matrix material, can have properties significantly different from those of the matrix. We have observed electrochemical, catalytic, and optical properties for nanostructure electrodes made of platinum nanoparticles in oxides [5,6]. The photoelectrochemical response of the nanophase composite,

which serves as an electrochromic material, was different from that of tungsten oxide due to presence of the platinum nanoparticles near the oxide matrix.

The routes for preparation of metallic low-dimensional systems have mainly been by wet chemical synthesis, template synthesis, and vapor–liquid–solid condensation [7–14]. In general, conventional sputtering deposition with a single sputtering target cannot easily produce unique nanostructured electrodes, due to the thin-film type growth mode in sputter deposition. However, cosputtering is a promising technique in that it can provide two-phase electrodes consisting of metal and oxide, because cosputtering uses two independent sputter guns for the metal and oxide materials. It has been shown that electrodes cosputtered from metal and oxide sputtering targets produce a metallic nanostructure within an oxide matrix [15,16]. The formation of the nanostructure within the oxide may be due to the oxide material limiting growth of deposited metallic phase. Accordingly, the size and shape of nanophase formed in oxide matrix can be controlled by experimental parameters such as the power of each target and the working gas pressure.

\* Corresponding authors. Tel.: +1 814 865 9121; fax: +1 814 865 3292.

E-mail addresses: [kup12@psu.edu](mailto:kup12@psu.edu) (K.-W. Park), [mftoney@slac.stanford.edu](mailto:mftoney@slac.stanford.edu) (M.F. Toney).

In this paper, we describe a nanostructure Ta<sub>2</sub>O<sub>5</sub>–Pt electrode fabricated by means of cosputtering and characterization of its structural and electrochemical properties. The Pt particles in the electrode had a worm-like shape of several nanometers in size as confirmed by both transmission electron microscopy (TEM) and small angle X-ray scattering (SAXS). The electrochromic properties of nanoworm-shaped Ta<sub>2</sub>O<sub>5</sub>–Pt electrode were observed and compared with thin-film Ta<sub>2</sub>O<sub>5</sub> electrodes.

## 2. Experimental

The nanoworm-shaped (Ta<sub>2</sub>O<sub>5</sub>–Pt) and thin-film (Ta<sub>2</sub>O<sub>5</sub>) electrodes were prepared using a sputtering system. Indium tin oxide (ITO) coated glass was used as transparent conducting substrate to observe electrochemical and electrochromic properties. The power of the Pt (20 W) and Ta<sub>2</sub>O<sub>5</sub> (60 W) sputtering guns was individually manipulated in order to fabricate a nanostructure electrode. The Ta<sub>2</sub>O<sub>5</sub> thin-film electrode was prepared using only the Ta<sub>2</sub>O<sub>5</sub> sputtering gun (60 W) to compare with Ta<sub>2</sub>O<sub>5</sub>–Pt. Sputtering was carried out under an atmosphere of Ar gas at 40 SCCM at room temperature. The base and working pressure were less than  $1 \times 10^{-6}$  and  $1 \times 10^{-2}$  Torr, respectively, for all films examined. Cu grids were also used as substrates for analysis by transmission electron microscopy (TEM). The TEM investigation was carried out using a Phillips CM20T/STEM Electron Microscope at an accelerating voltage of 200 kV. To confirm thickness of the sample, the cross-sectional images were observed by means of scanning electron microscopy (SEM, HITACHI S-4100). All the thickness of thin-film electrodes sputtered is  $\sim 20$  nm.

SAXS experiments were performed at the IMM-CAT at the Advanced Photon Source at Argonne National Laboratory. The incident X-rays from an undulator were monochromatized with a double-bounce Si(111) crystal to an energy of 6.6 keV. Slits confined the incidence beam size to either  $100 \times 100 \mu\text{m}$  (high resolution) or  $250 \times 250 \mu\text{m}$  (low resolution). An area detector was used with a sample to detector distance of either 3330 mm (high resolution) or 420 mm (low resolution). The samples were positioned with the substrate normal coinciding with the incident beam. To reduce attenuation from the substrate,  $\sim 80 \mu\text{m}$  Si substrates were used (which transmitted  $\sim 10\%$  of the incident beam). Since scattering from such thin films is inherently weak, great care was used to reduce contributions from background scattering. First, double-sided polished wafers were used to eliminate scattering emanating from the surface roughness of the substrate. Parasitic slit scattering from the beam defining slits was minimized through the use of slits with hemispherical polished blades and the careful placement of guard slits. Finally, the sample was placed

in vacuum and there were no windows between the beamstop and the beam defining slits (just after the monochromator). The SAXS data were background subtracted, circularly averaged, and normalized with respect to the transmitted beam intensity.

To characterize the electrochemical properties of electrodes, cyclic voltammetry was examined in 0.5 M H<sub>2</sub>SO<sub>4</sub> at a scan rate of  $20 \text{ mV s}^{-1}$ . The deposited thin-films were used as the working electrodes. All the actual surface area of the working electrodes is  $0.75 \text{ cm}^2$ . Pt gauze and Ag|AgCl (sat. KCl) were used as counter and reference electrodes, respectively. The potential is reported with respect to normal hydrogen electrode (NHE). The electrochemical measurements for the direct observation of electrochromism in the electrodes was done in an electrochemical cell with optics consisting of a 633 nm He–Ne laser as the light source and a power meter for detection of the optical signal modulation. During the electrochemical reaction with respect to the potential, the laser was transmitted through the thin-film electrode and the modulation of the signal intensity was continually detected. The electrochemical cell was comprised of Pt and Ag|AgCl as the counter and reference electrodes, respectively. The nanostructure and thin-film electrodes were used as the working electrodes in the electrochemical cell.

## 3. Results and discussion

As can be seen in the TEM image of Ta<sub>2</sub>O<sub>5</sub>–Pt in Fig. 1(a), the nanostructure electrode consists of worm-shaped Pt nanoparticles that are well dispersed in tantalum oxide. The Pt nanoparticles show worm-like shape of about 2 nm in a diameter and of 5–6 nm in a length. In spite of the fact that the thin-film electrode was fabricated using sputtering deposition, discrete nanostructures are formed in the amorphous oxide. The possible origin of the formation of the Pt nanoparticles with an amorphous oxide matrix may be as follows: (1) thermodynamically stable phase separation between metal and oxide; (2) prevention of migration of deposited metal ad-atoms by oxide matrix; and (3) spinoidal decomposition where one expects to form a random pattern with a characteristic length corresponding to the wavelength of the fastest growing fluctuations [17]. The size and shape of metallic nanophases in oxide matrix may be controlled by several experimental parameters such as oxide material, power of sputtering guns, and the working pressure and is presently being investigated. The diffraction pattern shown in the inset to Fig. 1 indicates the formation of Pt metallic nanostructures with crystallinity. In addition, as shown in Fig. 1(b), the high resolution TEM (HRTEM) image shows the formation of a worm-shaped Pt metallic structure in the amorphous tantalum oxide. The Fourier transform diffraction

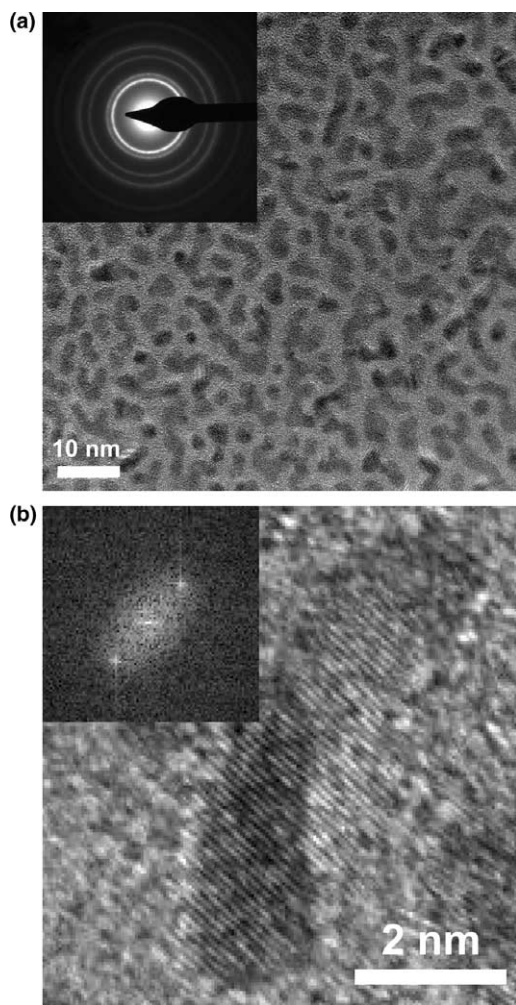


Fig. 1. (a) Transmission electron micrograph (TEM) images of nanoworm-shaped  $\text{Ta}_2\text{O}_5$ -Pt electrode (the inset in (a) shows the ring pattern of the electrode by transmission electron diffraction (TED)). (b) High-resolution TEM (HRTEM) image of nanoworm-shaped  $\text{Ta}_2\text{O}_5$ -Pt electrode.

pattern at the inset in Fig. 1(b) indicates a crystalline structure of the sputtered Pt within  $\text{Ta}_2\text{O}_5$ .

To further characterize the nanophase electrodes, we have utilized SAXS, a well-established technique that probes structural correlations for length scales of 1–100 nm [18,19]. SAXS data are shown by the open squares in Fig. 2 and are plotted as a function of the scattering vector,  $Q = (4\pi/\lambda)\sin(\theta)$ , where  $2\theta$  is the angle between the scattered photon and transmitted beam. The strong peak at about  $0.12 \text{ \AA}^{-1}$  shows that the positions of the Pt nanoparticles are correlated, while the width of this peak indicates substantial disorder in this correlation, as expected for sputter deposition. Apparent in the inset is a weaker peak at about  $Q = 0.2 \text{ \AA}^{-1}$ ; this is  $\sqrt{3}$  of the strong peak, as expected for two-dimensional (2D) hexagonal-close packing (hcp) of the wormlike Pt nanoparticles. The line in Fig. 2 shows a fit to the data assuming a 2D hcp arrangement of the Pt nanopar-

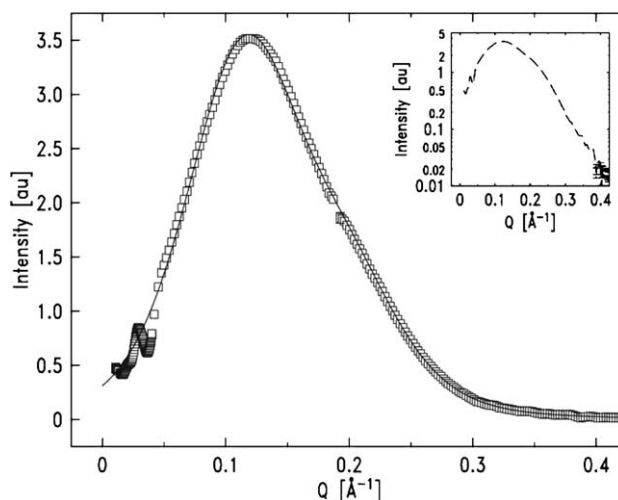


Fig. 2. SAXS data for  $\text{Ta}_2\text{O}_5$ -Pt electrode. The open symbols are the data, while the solid line is a best fit. The inset shows that data (dashed line) on a logarithmic scale, which makes the higher order peaks more apparent.

ticles. This is a valid model for wormlike nanoparticles, since the length of the nanoparticles is significantly larger than their radius. As is apparent, the model fits the data well. From this model, we find that the average spacing between the particles is 6 nm and that the average diameter is 2.2 nm, in good agreement with the TEM data of Fig. 1. Hence, the structural picture that emerges for the  $\text{Ta}_2\text{O}_5$ -Pt electrodes is one where the Pt nanoparticles phase separate in the  $\text{Ta}_2\text{O}_5$  matrix. As results of the sputtering conditions, the nanoparticles have a wormlike shape with a diameter of about 2 nm and a length of 5–6 nm. The spacing between the Pt worms is about 6 nm, but there is considerable disorder in this spacing.

The electrochemical properties of  $\text{Ta}_2\text{O}_5$ -Pt and  $\text{Ta}_2\text{O}_5$  electrodes were analyzed in 0.5 M  $\text{H}_2\text{SO}_4$  solution by means of cyclic voltammetry, as shown in Fig. 3. The cyclic voltammogram (CV) of the  $\text{Ta}_2\text{O}_5$ -Pt electrode at room temperature was obtained with a scan rate of  $20 \text{ mV s}^{-1}$ . The peaks for the reduction (Re(H)) and oxidation (Ox(H)) of hydrogen and oxidation (Ox(O)) and reduction (Re(O)) of oxygen on the Pt surface in  $\text{H}_2\text{SO}_4$  are clearly seen. Hence, the CV of the  $\text{Ta}_2\text{O}_5$ -Pt electrode demonstrates the presence of polycrystalline Pt. As also shown in Fig. 3, the  $\text{Ta}_2\text{O}_5$  exhibits an extremely low current density, and there is no reaction of  $\text{Ta}_2\text{O}_5$  in the potential range for the Pt-related electrochemical reactions such as hydrogen oxidation/reduction and oxygen oxidation/reduction.

Fig. 4 shows a variation of optical transmittance in electrodes ( $\text{Ta}_2\text{O}_5$  and  $\text{Ta}_2\text{O}_5$ -Pt) with respect to an applied potential. According to an electrochromism of cathodic coloration materials, an optical signal

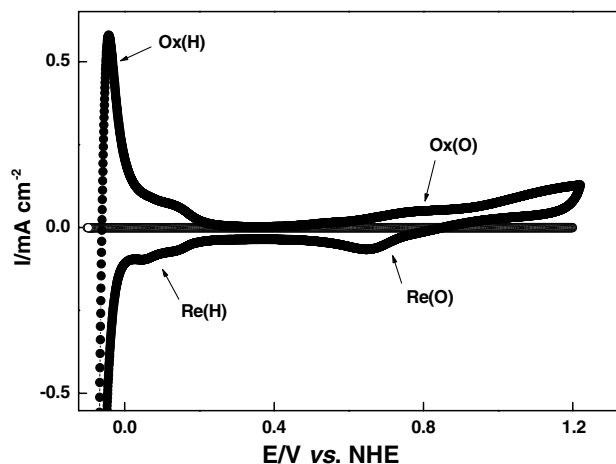


Fig. 3. Cyclic voltammogram of Ta<sub>2</sub>O<sub>5</sub>-Pt (●) and Ta<sub>2</sub>O<sub>5</sub> (○) electrodes in 0.5 M H<sub>2</sub>SO<sub>4</sub>.

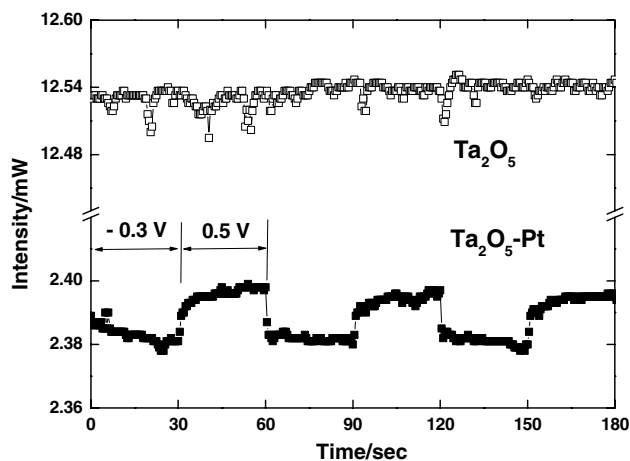


Fig. 4. Optical intensity modulation of Ta<sub>2</sub>O<sub>5</sub>-Pt (■) and Ta<sub>2</sub>O<sub>5</sub> (□) electrodes as a function of electrochemical cell potential (−0.3 to +0.5 V at interval of 0.5 s).

intensity would be reduced (colored) at negative potential versus normal hydrogen electrode (NHE) and increased (bleached) at positive potential versus NHE in parallel with the potential of the electrochemical cell. The sputtered Ta<sub>2</sub>O<sub>5</sub> electrode shows no change in intensity while the nanoworm-shaped Ta<sub>2</sub>O<sub>5</sub>-Pt electrode shows an optical signal modulation as a function of an applied potential. In general, during an electrochromic process, electrons are injected or extracted under an applied voltage and, at the same time, ions are moved uniformly into or out of the EC material for the balance of charge neutrality. However, it is likely that the Ta<sub>2</sub>O<sub>5</sub> electrode with a few nanometers in thickness has no sufficient electronic conductivity to produce an electrochemical motion and shows no electrochromic properties. On the other hand, the Ta<sub>2</sub>O<sub>5</sub>-Pt electrode with the same thickness as the Ta<sub>2</sub>O<sub>5</sub> electrode displays

an electrochromism of cathodic coloration materials. This indicates that an injection or extraction of electrons in the Ta<sub>2</sub>O<sub>5</sub>-Pt is affected by well-defined Pt polycrystalline nanostructures, thus enhancing proton transfer phenomenon, i.e., cathodic electrochromic properties of Ta<sub>2</sub>O<sub>5</sub>.

#### 4. Conclusions

The Ta<sub>2</sub>O<sub>5</sub>-Pt nanostructured electrode showed worm-like Pt crystalline nanoparticles in Ta<sub>2</sub>O<sub>5</sub> matrix as confirmed by transmission electron microscopy and small angle X-ray scattering. The Ta<sub>2</sub>O<sub>5</sub>-Pt nanostructured electrode displayed typical cathodic electrochromism compared to Ta<sub>2</sub>O<sub>5</sub> thin-film electrode with no electrochromism. Such an electrochromic phenomenon in the Ta<sub>2</sub>O<sub>5</sub>-Pt is likely due to the Pt crystalline nanostructure in a tantalum oxide material.

#### Acknowledgments

K.-W. Park acknowledges very helpful comments of Prof. Thomas E. Mallouk in Department of Chemistry, the Pennsylvania State University. The SAXS experiments were performed at the Advanced Photon Source at Argonne National Laboratory, which is supported by the US Department of Energy, Office of Science, Office of Basic Energy Sciences, under Contract No. W-31-109-ENG-38. Portions of this research were carried out at the Stanford Synchrotron Radiation Laboratory, a national user facility operated by Stanford University on behalf of the US Department of Energy, Office of Basic Energy Sciences.

#### References

- [1] A.P. Alivisatos, *Science* 271 (1996) 933.
- [2] Y. Cui, Q.Q. Wei, H.K. Park, C.M. Lieber, *Science* 293 (2001) 1289.
- [3] J. Johnson, P.K. Knutsen, H. Yan, M. Law, P. Yang, R. Saykally, *Nano Lett.* 4 (2004) 197.
- [4] T. Hyeon, *Chem. Commun.* 927 (2004).
- [5] K.-W. Park, Y.-E. Sung, *J. Appl. Phys.* 94 (2003) 7276.
- [6] K.-W. Park, K.-S. Ahn, J.-H. Choi, Y.-C. Nah, Y.-E. Sung, *J. Phys. Chem. B* 107 (2003) 4352.
- [7] E.M. Chan, R.A. Mathies, A.P. Alivisatos, *Nano Lett.* 3 (2003) 199.
- [8] M. Tian, J. Wang, J. Kurtz, T.E. Mallouk, M.H.W. Chan, *Nano Lett.* 3 (2003) 919.
- [9] J. Wang, M. Tian, T.E. Mallouk, M.H.W. Chan, *J. Phys. Chem. B* 108 (2004) 814.
- [10] M.S. Gudisken, M.C. Lieber, *J. Am. Chem. Soc.* 122 (2000) 8801.
- [11] M.S. Gudisken, L.J. Lauthon, J. Wang, D.C. Smith, M.C. Lieber, *Nature* 415 (2002) 617.
- [12] T. Kuykendall, P. Pauzauskie, S.K. Lee, Y. Zhang, P. Yang, *Nano Lett.* 3 (2003) 1063.

- [13] S.-W. Kim, J. Park, Y. Jang, Y. Chung, S. Hwang, T. Hyeon, *Nano Lett.* 3 (2003) 1289.
- [14] J. Joo, T. Yu, Y.W. Kim, H.M. Park, F. Wu, J.Z. Zhang, T. Hyeon, *J. Am. Chem. Soc.* 125 (2003) 6553.
- [15] K.-W. Park, K.-S. Ahn, J.-H. Choi, Y.-C. Nah, Y.-M. Kim, Y.-E. Sung, *Appl. Phys. Lett.* 81 (2002) 907.
- [16] K.-W. Park, K.-S. Ahn, J.-H. Choi, Y.-C. Nah, Y.-E. Sung, *Appl. Phys. Lett.* 82 (2003) 1090.
- [17] D.A. Porter, K.E. Eaterling, *Phase Transformations in Metals and Alloys*, CRC Press, Boca Raton, 1992.
- [18] E. Huang, M.F. Toney, L.B. Lurio, W. Volksen, D. Mecerreyes, P. Brock, H.-C. Kim, C.J. Hawker, J.L. Hedrick, V.Y. Lee, T. Magbitang, R.D. Miller, *Appl. Phys. Lett.* 81 (2002) 2232.
- [19] M.F. Toney, K.A. Rubin, S.-M. Choi, C.J. Glinka, *Appl. Phys. Lett.* 82 (2003) 3050.